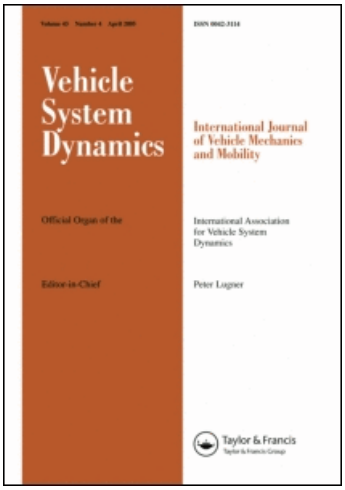

Vehicle System Dynamics
Publication details, including instructions for authors and subscription information:
http://www.informaworld.com/smpp/title~content=t713659010

Fault-tolerant control of heavy-haul trains

Xiangtao Zhuan [ab];Xiaohua Xia [ab]
[a] Department of Electrical, Electronic and Computer Engineering, University of Pretoria, Pretoria, South Africa [b] Department of Automation, Wuhan University, Wuhan, China

First published on: 21 October 2009

To cite this Article Zhuan, Xiangtao andXia, Xiaohua(2010) 'Fault-tolerant control of heavy-haul trains', Vehicle System Dynamics, 48: 6, 705 — 735, First published on: 21 October 2009 (iFirst)
To link to this Article: DOI: 10.1080/00423110902974100
URL: http://dx.doi.org/10.1080/00423110902974100

Vehicle System Dynamics
Vol. 48, No. 6, June 2010, 705–735

Taylor & Francis
Taylor & Francis Group

Fault-tolerant control of heavy-haul trains

Xiangtao Zhuan[a,b]* and Xiaohua Xia[a,b]

[a]*Department of Electrical, Electronic and Computer Engineering, University of Pretoria, Pretoria 0002, South Africa;* [b]*Department of Automation, Wuhan University, Wuhan 430072, China*

(*Received 1 August 2008; final version received 15 April 2009; first published 21 October 2009*)

The fault-tolerant control (FTC) of heavy-haul trains is discussed on the basis of the speed regulation proposed in previous works. The fault modes of trains are assumed and the corresponding fault detection and isolation (FDI) are studied. The FDI of sensor faults is based on a geometric approach for residual generators. The FDI of a braking system is based on the observation of the steady-state speed. From the difference of the steady-state speeds between the fault system and the faultless system, one can get fault information. Simulation tests were conducted on the suitability of the FDIs and the redesigned speed regulators. It is shown that the proposed FTC does not explicitly worsen the performance of the speed regulator in the case of a faultless system, while it obviously improves the performance of the speed regulator in the case of a faulty system.

Keywords: fault detection and isolation; fault tolerant control; nonlinear system; measurement feedback; heavy-haul train

1. Introduction

For the control strategies of train handling, various studies have been carried out, such as in [1–5]. In [1,2], some kinds of open-loop control are proposed while in [3–5], some kinds of closed-loop control are developed on the basis of state feedback. Recently, a nonlinear system theory approach, output regulation of nonlinear systems is given in [6] for train handling on the basis of measurement feedback. In these papers, however, all the controllers are designed on the assumption that the train is well set up and all the actuators (supplying traction efforts and braking efforts of locomotives and wagons) and sensors work as designed, which is an ideal condition. In practice, some of the actuators and/or sensors may be faulty, and even worse, the train structure may be changed. For example, the speed sensor has a constant bias, or the amplifier in the sensor circuit has a fault which leads to a gain fault of the sensor. The locomotive may fail during the operation, which happened in the ECP trial run to collect data to validate the cascade-mass-point model in [7] on 18 November 2003. In the trial run, one of the two front locomotives was faulty such that one could not make any effort for a section of the track. The air pressure in the braking pipe may be different from expected because of a fault in

*Corresponding author. Email: xtzhuan@whu.edu.cn

ISSN 0042-3114 print/ISSN 1744-5159 online

DOI: 10.1080/00423110902974100
http://www.informaworld.com

the pressure sensor in the air recharge system or air leakage, which makes the braking forces acting on the wheels less than expected. When a fault happens, the controller, designed on the basis of the faultless train model, cannot work as well as expected, and sometimes it even leads to unsafe running, such as train-breaking and derailment, i.e., the safe running of trains cannot be guaranteed. Some safe running methods are therefore necessary in train handling. Actually, in some fault modes of train handling, it is possible to assure train performance with suitably redesigned controllers.

In nature, the above-mentioned controller redesign is a fault-tolerant control (FTC) problem. In the literature, there are many papers about such problems. Some survey papers, such as [8–15], provide excellent reviews on the subject of FTC. For linear systems, geometric approaches are proposed for fault detection and isolation (FDI), for example, in [16–18]. A combined input–output and local approach is proposed in [19] for the problem of FDI of nonlinear systems modelled by polynomial differential-algebraic equations. A high-gain observer-based approach for FDI of an affine nonlinear system is advanced in [20], where a sufficient condition is given. In [21], a geometric approach to FDI of nonlinear systems is proposed, while a necessary condition for the existence of FDI is exploited based on a geometric concept–*unobservability distribution* introduced by the authors in [22]. For the solution of FDI, a sufficient condition is also given. A stability- and performance-vulnerable failure of sensors can be identified with the approach in [23] for nonlinear systems. The switch between two robust control strategies based on normal operation and faulty operation is used to realise FTC. An information-based diagnostic approach is investigated in [24] for a class of SISO nonlinear system in a triangular structure. In [25], a fault diagnosis approach is proposed based on adaptive estimation by combining a high-gain observer and a linear adaptive observer. As is known, the high-gain observer is sensitive to measurement noise. In speed regulation of heavy-haul trains with measurement (speeds) feedback, noise is inevitable, so a high-gain observer is not considered in this study. Recently, compared with [21], a relaxed formulation of FDI of nonlinear systems is proposed in [26], where a residual generator has been designed to detect a set of faults.

In train handling, such problems have been investigated in [27,28] for some kinds of faults with induction motors. The FDI of diesel engines are seen in [29,30]. Paper [28] is in essence on FTC of the induction motor, which can also be seen in [31]. In [32], some brief results of FTC of heavy-haul trains are shown. In this paper, the FTC of the whole train is studied for the actuator faults and sensor faults. The faulty modes of a train include the gain faults of speed sensors, the locomotive actuators (induction motors, in this study), and wagon actuators (the braking systems). The locomotive fault signal is assumed to be acquired from other FDIs and is available in its fault-tolerant controller redesign. Based on the train model and fault modes, a fault-tolerant speed regulator (including the FDI part and FTC part) is designed for the faults of sensors and braking systems, respectively. The fault-tolerant speed regulator of sensors' faults is based on the approach in [21], while the fault-tolerant speed regulator of the braking system fault is based on the steady-state calculation. With the fault signals of FDIs, the speed regulator in [6] can be suitably redesigned to maintain the train's performance.

In this study, Simulation tests are conducted to show the suitability of the FTC. Simulation results show that the application of the proposed FTC does not explicitly worsen the performance of the speed regulator in the case of a faultless system while it obviously improves the performance of the speed regulator in the case of a faulty system.

The structure of this paper is as follows: The train model and fault modes are given in Section 2. Fault detection and isolation are studied in Section 3 while the corresponding FTC are discussed in Section 4. Simulation results are shown in Section 5. Some conclusions are made in Section 6.

2. Fault modes of heavy-haul trains

A cascade-mass-point model for a heavy-haul train is shown in Figure 1, and the longitudinal dynamics are given in [33] as follows:

$$\begin{aligned} m_i\dot{v}_i &= u_i + f_{\text{in}_{i-1}} - f_{\text{in}_i} - f_{a_i}, \quad i = 1, \ldots, n, \\ \dot{x}_j &= v_j - v_{j+1}, \quad j = 1, \ldots, n-1, \end{aligned} \tag{1}$$

where the variable m_i is the ith car's mass, the variables v_i, u_i are the speed and control effort (traction force or dynamic braking force for a locomotive and the braking force for a wagon) of the ith car. The variable $f_{a_i} = f_{\text{aero}_i} + f_{p_i}$, $i = 1, 2, \ldots, n$ are the forces undertaken by the cars from the environment, where $f_{\text{aero}_i} = m_i(c_{0_i} + c_{1_i}v_i + c_{2_i}v_i^2)$ is the ith car's aerodynamic force, the variable $f_{p_i} = f_{g_i} + f_{c_i}$ is the force due to the track slope and curvature where the ith car is running. The variable f_{in_i} is the in-train force between the ith and $(i+1)$th cars, which is a function of x_i, the relative displacement between the two neighbouring cars, and the difference of the neighbouring cars' velocities (damping effect). The variables $c_{0_1}, c_{1_i}, c_{2_i}$ are constants. In Equation (1), one has $f_{\text{in}_0} = f_{\text{in}_n} = 0$.

With open-loop scheduling, one can get the equilibria $f^0_{\text{in}_j}(x^0_j)$, $v^0_i(v_r)$, u^0_i, $j = 1, 2, \ldots, n-1$, $i = 1, 2, \ldots, n$, which are the in-train forces (static displacement of coupler), the speeds (reference speed), and the traction/braking forces. Then a difference system between the train model and the equilibria is as

$$\begin{aligned} \delta\dot{v}_s &= (\delta u_s + \delta f_{\text{in}_{s-1}} - \delta f_{\text{in}_s} - \delta f a_s)/m_s, \\ \delta\dot{x}_j &= \delta v_j - \delta v_{j+1}, \quad s = 1, \ldots, n, \quad j = 1, \ldots, n-1, \end{aligned} \tag{2}$$

where $\delta v_s = v_s - v_s^0 = v_s - v_r$, $\delta u_s = u_s - u_s^0$, $\delta f_{\text{in}_s} = f_{\text{in}_s} - f^0_{\text{in}_s}$, $\delta x_j = x_j - x_j^0$.

The above system can be rewritten as

$$\begin{aligned} \delta\dot{v} &= f_{11}(\delta v) + A_{12}\delta x + Bu, \\ \delta\dot{x} &= A_{21}\delta v, \end{aligned} \tag{3}$$

where $\delta v = [\delta v_1, \ldots, \delta v_n]^{\text{T}}$, $\delta x = [\delta x_1, \ldots, \delta x_{n-1}]^{\text{T}}$, $f_{11}(\delta v) = [f^1_{11}(\delta v_1), \ldots, f^n_{11}(\delta v_n)]^{\text{T}}$ in which $f^i_{11}(\delta v_i) = (c_{1_i} + 2c_{2_i}v_r)\delta v_i + 2c_{2_i}\delta v_i^2$,

$$B = \text{diag}\left(\frac{1}{m_1}, \ldots, \frac{1}{m_n}\right),$$

$$A_{12} = \begin{bmatrix} -\dfrac{k_1}{m_1} & 0 & \cdots & 0 & 0 \\ \dfrac{k_1}{m_2} & -\dfrac{k_2}{m_2} & \cdots & 0 & 0 \\ \cdots & \cdots & \cdots & \cdots & \cdots \\ 0 & \cdots & 0 & \dfrac{k_{n-2}}{m_{n-1}} & -\dfrac{k_{n-1}}{m_{n-1}} \\ 0 & \cdots & 0 & 0 & \dfrac{k_{n-1}}{m_n} \end{bmatrix}$$

$$A_{21} = \begin{bmatrix} 1 & -1 & 0 & \cdots & 0 & 0 \\ 0 & 1 & -1 & \cdots & 0 & 0 \\ \cdots & \cdots & \cdots & \cdots & \cdots & \cdots \\ 0 & 0 & 0 & \cdots & 1 & -1 \end{bmatrix}.$$

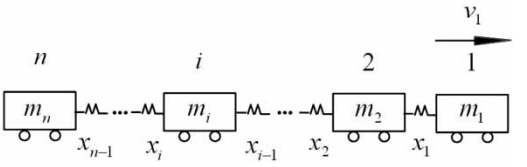

Figure 1. The longitudinal dynamics of a heavy-haul train.

The variables $k_i,\ i=1,\ \ldots,n-1$ are chosen to be constant. In the following, one also denotes $A_{11}=\partial f_{11}(0)/\partial\delta v$.

In this study, the fault modes include speed-senor faults and actuator faults.

2.1. *Speed-sensor faults*

The states of a train include the speeds of cars and the relative displacement of the couplers (in-train forces). It is very difficult to measure the relative replacements directly; however, the speeds of the cars could be measured directly when the cars are equipped with speed sensors. Here analogue tachometers with 4–20 mA output are assumed to be employed for speed measurement. There is an electric circuit for the data sampling of 4–20 mA current. The current flows through a resistor with a resistance of 250 Ω, and the measurement of the current could be done through the measurement of voltage across the resistor. The electric circuit for the 4–20 mA signal to be sampled by a controller includes at least an amplifier. For such a kind of tachometers, the measurement is inevitably influenced by the environment, such as temperature, moisture, electro-magnetic environment, and so on. Thus the accuracy of the resistor and the operation of the amplifier will affect the measurement of speed, and even lead to the gain fault of speed measurement. The gain fault could be negative or positive.

The speed sensor may be faulty with a constant bias, and/or with a gain fault due to the gain change of the amplifier in the circuit. In the former case, such a fault can be corrected by the calibration before its application. In this paper, the latter case is considered; that is, the sensor for the ith car's speed is faulty with a gain fault,

$$v_i = (1+m_{v_i}^f)v_i^o, \tag{4}$$

where the variable v_i is the sensor output for the ith car's speed, v_i^o is the real speed, and $m_{v_i}^f$ is the constant gain fault of the sensor.

Assuming there are q sensors equipped for q cars of the train, and they are located at the positions $ls_1,\ \ldots,ls_q$. Then, the dynamics of a train with speed measurement (3) is as follows:

$$\begin{aligned}\delta\dot{v} &= f_{11}(\delta v)+A_{12}\delta x+Bu,\\ \delta\dot{x} &= A_{21}\delta v,\\ y_i &= (1+m_{v_{ls_i}}^f)v_{ls_i}-v_r,\quad i=1,\ldots,q,\end{aligned} \tag{5}$$

where $m_{v_{ls_i}}^f$ is a constant gain fault of the ith sensor, and y_i is the speed measurement.

2.2. *Actuator faults*

The actuators of a train include the locomotives' engines (traction efforts or dynamic braking forces) and the wagons' brakes (braking efforts). However, the actuators are sometimes faulty.

For example, one locomotive in a locomotive group (composed of n_l locomotives) does not work, then the actual output of the locomotive group is $n_l - 1/n_l$ of the expected. The air pressure in the braking pipe is sometimes different from the designed one owing to air leakage or a fault of the pressure sensor in the air recharging system, which leads to less braking effort in the braking system. In train handling, every locomotive has its own engine, whose running condition is independent of the others while all wagons share the same braking pressure in the air pipe along the train, whose fault leads to the same faults on all wagons.

In the above cases, the outputs of the actuators may not be equal to those expected, but proportional to the expected ones, i.e.,

$$u_i^f = (1 - m_f^i)u_i, \quad i = 1, \ldots, n, \tag{6}$$

in which u_i and u_i^f is expected output and real output, respectively. The last one includes the open-loop part u_i^o and the closed-loop part U_i. The coefficient m_f^i is a fault coefficient. In Equation (6),

$$0 \leq m_f^i \leq 1.$$

In the following analysis, one assumes that the locomotives' faults are independent and the wagons' faults are the same, i.e.,

$$\begin{aligned} u_{l_i} &= (1 - m_f^{l_i})u_{l_i}, \quad i = 1, \ldots, k, \\ u_j &= (1 - m_f^w)u_j, \quad j = 1, \ldots, n,\ j \neq l_i. \end{aligned} \tag{7}$$

3. Fault detection and isolation

3.1. *Sensor FDI*

The sensors involved in train handling are the speed sensors. When the faults of these sensors are considered and viewed as pseudo-actuators, the train model described in Equation (5) is as follows:

$$\begin{aligned} \delta\dot{v} &= f_{11}(\delta v) + A_{12}\delta x + BU, \\ \delta\dot{x} &= A_{21}\delta v, \\ \dot{v}_{ls_i}^f &= -v_{ls_i}^f + u_{ls_i}^f v_{ls_i}, \\ y_i &= \delta v_{ls_i} + v_{ls_i}^f, \quad i = 1, \ldots, q, \end{aligned} \tag{8}$$

where $u_{ls_i}^f$ are pseudo-actuators of sensor faults.

In [6], it is assumed that there is a speed sensor for the first car (usually a locomotive). It is convenient to assume that this sensor is always in good condition and the output of this sensor is y_1, which can be guaranteed by some hardware structures, for example, a hardware redundancy. With this assumption, for every sensor fault mode (the output of this sensor is $y_i, i = 2, \ldots, q$), the train is modelled as

$$\begin{aligned} \delta\dot{v} &= f_{11}(\delta v) + A_{12}\delta x + BU, \\ \delta\dot{x} &= A_{21}\delta v, \\ \dot{v}_{ls_i}^f &= -v_{ls_i}^f + u_{ls_i}^f v_{ls_i}, \\ y_1 &= \delta v_1, \\ y_i &= \delta v_{ls_i} + v_{ls_i}^f, \quad i = 2, \ldots, q. \end{aligned} \tag{9}$$

When the ith fault $u^f_{ls_i}$ is considered as a fault signal to be detected, the other faults ($u^f_{ls_j}$, $j \in [2, q]$, $j \neq i$) are thought as disturbance to be decoupled.

For Equation (9), assuming the co-distribution $\Theta = \Omega_0$ ($\Omega_0 = \text{span}\{d(\delta v_1), \ldots, d(\delta v_n), d(\delta x_1), d(\delta x_{n-1})\}$) in the observability co-distribution algorithm in [21], one has,

$$\begin{aligned}
Q_0 &= \Omega_0 \cap \text{span}\{dh\} = \text{span}\{\text{d}(\delta v_1)\},\\
Q_1 &= \Omega_0 \cap \bar{Q}_0 = \text{span}\{\text{d}(\delta v_1), \text{d}(\delta x_1)\},\\
Q_2 &= \Omega_0 \cap \bar{Q}_1 = \text{span}\{d(\delta v_1), \text{d}(\delta v_2), \text{d}(\delta x_1)\},\\
&\vdots\\
Q_{2n-1} &= \text{span}\{d(\delta v_1), \ldots, d(\delta v_{n-1}), d(\delta x_1), \ldots, d(\delta x_{n-1})\},\\
Q_{2n} &= \text{span}\{d(\delta v_1), \ldots, d(\delta v_n), d(\delta x_1), \ldots, d(\delta x_{n-1})\},
\end{aligned}$$

and o.c.a(Ω_0) = Ω_0. From this co-distribution, it is easy to justify that the following co-distribution

$$\Omega = \text{span}\{d(\delta v_1), \ldots, d(\delta v_n), d(\delta x_1), d(\delta x_{n-1}), d(v^f_{ls_j})\}, \quad \forall j \in [2, q], \tag{10}$$

satisfies o.c.a.(Ω) = Ω.

Furthermore, one has

$$L_{g_j}\Omega \subset \Omega = \Omega + \text{span}\{dh\}, \quad \forall j \in [0, m]. \tag{11}$$

The conditions of an observability co-distribution in [21] are satisfied, i.e., Ω is an observability co-distribution.

It is obvious that the vector field $p_j, j \in [2, p], j \neq i$ is in the annihilator of Ω while $\text{span}\{l\} \subset \Omega$. So it is possible to transform the train dynamics with sensor faults (9) into the form of Equation (38) in [21], which means the possibility of fault detection of ith sensor fault.

A residual generator for the ith sensor can be in the following form:

$$\begin{aligned}
\dot{\xi}_1 &= f_{11}(\xi_1) + A_{12}\xi_2 + BU + L_{11}(y_1 - \xi_{11}) + L_{13}(y_i - \xi_{1,ls_i}),\\
\dot{\xi}_2 &= A_{21}\xi_1 + L_{21}(y_1 - \xi_{11}) + L_{23}(y_i - \xi_{1,ls_i}),\\
\dot{\xi}_3 &= -\xi_3 + L_{31}(y_1 - \xi_{11}) + L_{33}(y_i - \xi_{1,ls_i}),\\
r_i &= (y_i - \xi_{1,ls_i})/(v_r + \xi_{1i}), \quad i \in [2, p],
\end{aligned}$$

where $\xi_1 = \text{col}(\xi_{11}, \ldots, \xi_{1n}) \in R^n$, $\xi_2 = \text{col}(\xi_{21}, \ldots, \xi_{2,n-1}) \in R^{n-1}$, $\xi_3 \in R$.

Especially, when $L_{13} = 0, L_{23} = 0$, it is also possible for the above form of dynamics to be a residual generator, because the original system with only the measurement of the first locomotive speed is also observable, which has been proved in [6]. It is very interesting to observe that this residual generator is naturally a fault identifier because the fault signal does not affect the states ξ_1, ξ_2, and the residual signal is actually the identifier signal of the fault. Furthermore, in this way, the residual generators and identifiers of all the sensor faults can share the same dynamics with different outputs, i.e.,

$$\begin{aligned}
\dot{\xi}_1 &= f_{11}(\xi_1) + A_{12}\xi_2 + BU + L_{11}(y_1 - \xi_{11}),\\
\dot{\xi}_2 &= A_{21}\xi_1 + L_{21}(y_1 - \xi_{11}),
\end{aligned} \tag{12}$$

and the output (a residual generator as well as a identifier) for the ith sensor fault is

$$r_i = \frac{y_2 - \xi_{1i}}{\xi_{1i} + v_r}. \tag{13}$$

3.2. *Actuator FDI*

A locomotive group effort is sometimes not the same as the expected one for some reasons, such as one locomotive of the locomotive group not working. The braking efforts of wagons may be different from the expected, because of the pressure change in the braking pipe. In the following, only the fault modes as in Equation (6) are studied.

When this happens, the efforts of the cars are proportional to the expected; that is, the fault mode described in Equation (7) is repeated as follows:

$$\begin{aligned} \delta\dot{v} &= f_{11}(\delta v) + A_{12}\delta x + BU + B_f(U + u^o), \\ \delta\dot{x} &= A_{21}\delta v, \end{aligned} \tag{14}$$

where

$$B_f = \operatorname{diag}\left(\frac{m_f^{l_1}}{m_1}, \overbrace{\frac{m_f^w}{m_2}, \ldots, \frac{m_f^w}{m_{n-1}}}^{n-2}, \frac{m_f^{l_2}}{m_n} \right).$$

To detect the actuators' faults, some states are assumed to be measurable. In this study, the train is assumed to be composed of n cars with one locomotive (group) at the front and one at the rear. The wagons are between these two locomotives (locomotive groups). The speeds of the two locomotives and the two wagons next to the locomotives are also available, i.e.,

$$y = \begin{bmatrix} v_1 \\ v_2 \\ v_{n-1} \\ v_n \end{bmatrix}. \tag{15}$$

The two kinds of fault modes (sensor fault and actuator fault) are studied separately, because there are some difficulties in studying these two kinds of faults simultaneously, which will be discussed later. So, in the study of actuator faults, the speed sensors are assumed to be in good condition.

3.2.1. *Locomotive FDI*

The locomotive group fault diagnosis is not studied in this paper. Some approaches may be used to supervise the running states of the locomotives, such as in [27–31]. In this study, the fault signals are assumed to be given, and when a fault happens, one's task is to redesign the controller.

3.2.2. *Wagon FDI*

When the wagon faults in system (14) are concerned, based on the geometric approach in [21], the wagon fault may be detected with a suitable residual generator. However the dimension of the residual generator is $2n-4$. For a long train, n is very large. To avoid such a high-dimension observer, one considers another approach to identify the wagons' faults. The full train model is repeated as follows:

$$\begin{aligned} m_i\dot{v}_i &= (1 - m_f^i)u_i + f_{\mathrm{in}_{i-1}} - f_{\mathrm{in}_i} - f_{p_i} \\ &\quad - m_i(c_{0_i} + c_{1_i}v_i + c_{2_i}v_i^2), \quad i = 1, \ldots, n, \\ \dot{x}_j &= v_j - v_{j+1}, \quad j = 1, \ldots, n-1. \end{aligned} \tag{16}$$

When $m_f^i = 0$, one has reached an equilibrium (steady state, $\dot{v} = 0, \dot{x} = 0$) $v_i = v_r, i = 1, \ldots, n,$ and $f_{\text{in}_i}^0(x_i^0)$, with $u_i = u_i^0$.

$$\begin{aligned} \dot{v}_r &= u_i^0 + f_{\text{in}_{i-1}}^0 - f_{\text{in}_i}^0 - f_{p_i} \\ &\quad - m_i(c_{0_i} + c_{1_i} v_r + c_{2_i} v_r^2), \quad i = 1, \ldots, n, \\ \dot{x}_j^0 &= v_r - v_r, \quad j = 1, \ldots, n-1. \end{aligned} \tag{17}$$

Thus one has a difference system (3), which is also denoted as follows:

$$\dot{X} = f(X) + BU. \tag{18}$$

A speed regulator designed in [6] for this difference system is as follows:

$$\begin{aligned} \dot{z} &= f(z) + BU + G_1(y_m - C_m z), \\ U &= c(w) + K(z - \pi(w)), \end{aligned} \tag{19}$$

The closed-loop dynamics is

$$\begin{aligned} \dot{X} &= f(X) + BU, \\ \dot{z} &= f(z) + BU + G_1(y_m - C_m z), \\ U &= c(w) + K(z - \pi(w)). \end{aligned} \tag{20}$$

When the train is faultless, its speed will track the reference speed under the controller (19). When $m_f^i \neq 0$, how is the train's dynamics? One first checks whether the train dynamics is stable. If it is, then one will study the new steady states.

The locomotives' faults are assumed to be detected and isolated through other approaches; so only the wagon faults with $m_f^i = m_f^w, i = 2, \ldots, n-1$ are considered in the identification.

When $m_f^w \neq 0$, the closed-loop dynamics (20) in cruise phase is as follows:

$$\begin{aligned} \dot{X} &= f(X) + BU + B_f(U + u^o), \\ \dot{z} &= f(z) + BU + G_1(y_m - C_m z), \\ U &= Kz, \end{aligned} \tag{21}$$

where

$$B_f = \operatorname{diag}\left(0, \overbrace{\frac{m_f^w}{m_2}, \ldots, \frac{m_f^w}{m_{n-1}}}^{n-2}, \overbrace{0, \ldots, 0}^{n}\right).$$

Assuming $A = \partial f(0)/\partial X,$ (from the above, one knows $A + BK < 0, A + G_1 C_m < 0$) one has a linearised model as follows:

$$\begin{aligned} \dot{X} &= AX + (B + B_f)Kz + B_f u^o, \\ \dot{z} &= -GC_m X + (A + G_1 C_m + BK)z. \end{aligned} \tag{22}$$

If the K, G are chosen such that

$$\begin{bmatrix} A & (B + B_f)K \\ -GC & A + GC + BK \end{bmatrix} < 0,$$

then the above system (22) is stable.

The steady state of the train can be denoted as $(\dot{v} = 0, \dot{x} = 0)v_i = v_r^f, i = 1, \ldots, n$, and $f_{\text{in}_i}^f(x_i^f)$, with u_i,

$$\begin{aligned}
\dot{v}_r^f &= u_1 - f_{\text{in}_1}^f - m_1(c_{0_1} + c_{1_1}v_r^f + c_{2_1}(v_r^f)^2) - f_{p_1},\\
\dot{v}_r^f &= u_i + f_{\text{in}_{i-1}}^f - f_{\text{in}_i}^f - m_i(c_{0_i} + c_{1_i}v_r^f + c_{2_i}(v_r^f)^2) - f_{p_i} - m_f^i u_i, \quad i = 2, \ldots, n-1,\\
\dot{v}_r^f &= u_n + f_{\text{in}_n}^f - m_n(c_{0_n} + c_{1_n}v_r^f + c_{2_n}(v_r^f)^2) - f_{p_n}.
\end{aligned} \tag{23}$$

If v_r^f is known, then there are only n unknown variables $f_{\text{in}_i}^f, i = 1, \ldots, n-1, m_f^w$ in the above n equations. Especially when summing up the equations, one has

$$\sum_{i=1}^{n} u_i - \sum_{i=1}^{n} m_i(c_{0_i} + c_{1_i}v_r^f + c_{2_i}(v_r^f)^2) = \sum_{j=2}^{n-1} m_f^i u_i. \tag{24}$$

It is possible to solve them, which means the identifiability of the wagon fault.

Although it is impossible for a train to reach steady states in practical running, it is practical to assume that the train can approximate its steady state, at least within a cruise phase. The practical steady-state speed of the running train is defined with the analysis of differences of the measurable speeds (v_1, v_2, v_{n-1}, v_n) in this paper.

When all the wagons are faultless and the train is running in its steady state, one has,

$$0 = \sum_{i=1}^{n} u_i^o - \sum_{i=1}^{n} m_i(c_{0_i} + c_{1_i}v_r + c_{2_i}(v_r)^2). \tag{25}$$

With Equations (24) and (25), if all the wagons' faults are the same, i.e., $m_f^i = m_f^w, i = 2, \ldots, n-1$, one has

$$(1 - m_f^w)\sum_{i=1}^{n} u_i - \sum_{i=1}^{n} u_i^o = \sum_{i=1}^{n} m_i(c_{1_i}v_r^f + c_{2_i}(v_r^f)^2 - (c_{1_i}v_r + c_{2_i}v_r^2)),$$

from which one can get m_f^w.

4. Fault-tolerant control

4.1. *FDI and FTC in the case of sensor faults*

The residual generator in the case of sensor faults is as in Equations (12) and (13), where function f_{11} is linearised and thus the observer is a linear system. The matrices L_{11}, L_{21} are determined through the function *LQR* in MATLAB. If the sensor fault model is linearised as

$$\begin{aligned}
\dot{z} &= Az + BU,\\
y_m &= C_m z,\\
y_i &= (1 + m_{v_i}^f)v_i - v_r, \quad i = 2, \ldots, p,
\end{aligned} \tag{26}$$

then one assumes $C_{m1} = C_m(1, :)$, $Q = I_{(2n-1)}$, $R = 1$, and with $L = lqr(A', C_{m1}', Q, R)$, $L = L'$, one gets the residual generator.

In FTC, one assumes the outputs of the residual generator are $\bar{v}_i$ and the measured speeds v_{mi}. The reference speed is v_r. In the control process, for the output v_{mi} of the ith speed

sensor, one will take $K_i^{\text{sensor}} \times v_{mi}$ as the real speed of the corresponding car, where K_i^{sensor} is a coefficient, which will be modified when the sensor fault is detected and isolated. A constant V_{th} is set as the threshold of fault diagnosis. For the FDI, one has other arrays in the program, $KD_{i,1:11}^{\text{sensor}}, N_i^{\text{sensor}}$. The former is used to store the past 11 coefficients of the sensor and the latter the times of violations of the fault-free condition.

The FDI program is shown in Figure 2, where $KD_{i,1:11}^{\text{sensor}} = 0_{1\times 11}, N_i^{\text{sensor}} = 0$ and $K_i^{\text{sensor}} = 1$ are initialised. This program is executed once a second.

It is known that there is a possibility of false rejections and a possibility of false acceptances for a fault-tolerant controller, which should be considered. The first possibility is that it does not detect or isolate the fault well when a fault occurs. The second is that it takes a faultless system as a fault system. The choice of the thresholds affect these two possibilities. Generally, when one possibility is reduced with a set of thresholds, the other one is increased. When the threshold is to be determined, the balance between the two possibilities should be considered.

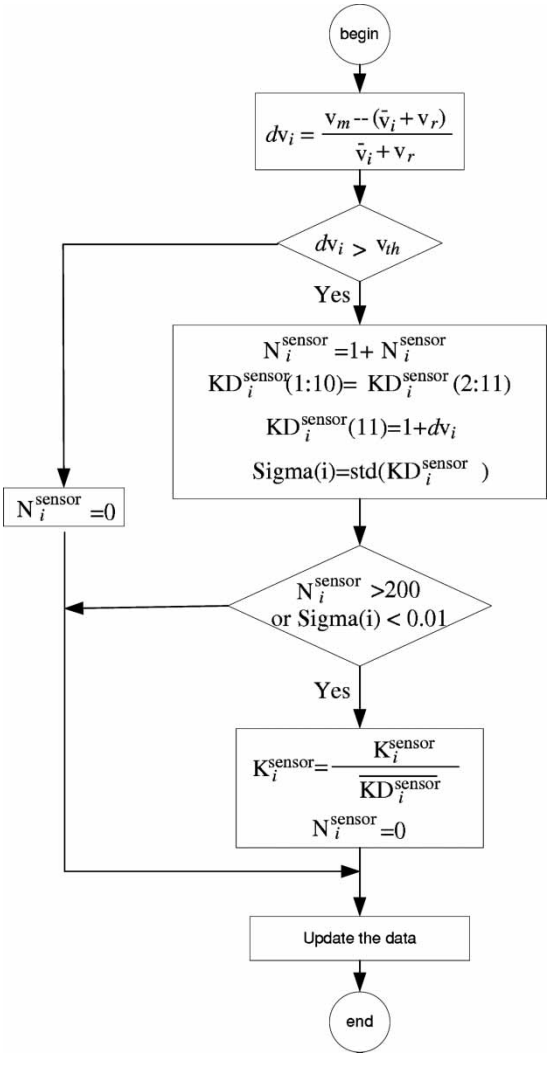

Figure 2. Sensor fault detection and isolation program.

From Figure 2, it is impossible to avoid the above two possibilities. However, the effects of the possibility of false acceptance can be discussed qualitatively. If a fault is falsely accepted, for example, a sensor with a gain 1 is falsely identified with a gain 1.05, then with the FTC, the speed of the train will be underestimated, and thus the train will be overspeed. In that case, the FDI will further identify a gain fault lower than 1 to correct the false acceptance. It is in the way of 'negative feedback' to track the real value of the gain. Such an approach in Figure 2 does not obviously affect the train performance. That can be seen from the simulation results of an FTC in a faultless system.

In this paper, the two possibilities from theoretic viewpoints will not be discussed, nor will the time delay between the fault occurrence and fault isolation. Instead, they will be discussed on the basis of the simulation results.

4.2. *FTC in the case of a locomotive fault*

As described before, FDI of locomotive faults are not studied in this study. Here, only the FTC of a locomotive fault is considered.

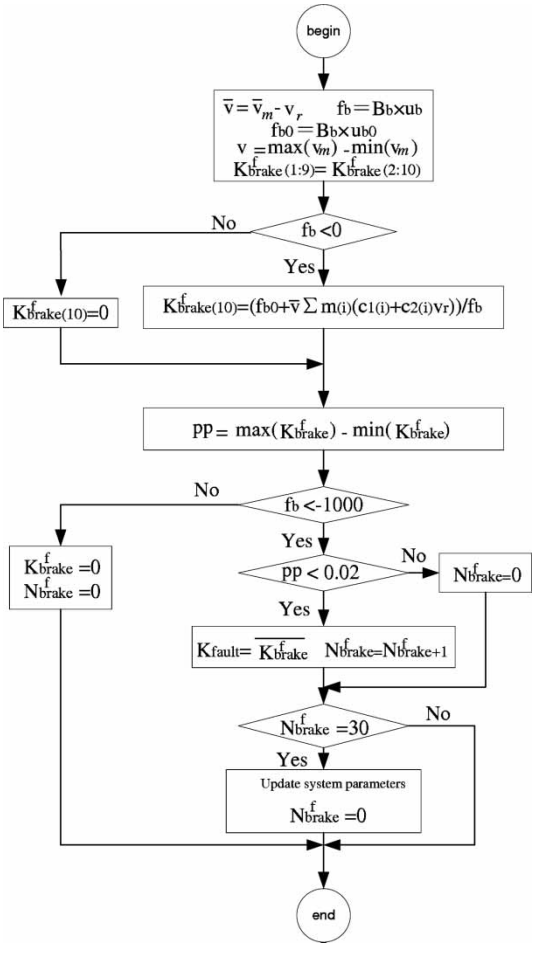

Figure 3. Wagon fault detection and isolation program.

In the following simulation, one assumes that the fault is detected and identified 60 s after it occurs. When it is identified, the controller will be redesigned. According to the fault, the parameters of the train are modified and then the controller is redesigned with the new parameters. For example, assuming the coefficient of its input in the train model is $Bt(i,:)$, if the locomotive group $u(i)$ loses half of its effort, the new coefficient is $Bt(i,:)/2$.

4.3. *FDI and FTC in the case of a wagon fault*

When a wagon fault is detected and identified, similar to the case of a locomotive fault, the controller will be redesigned according to the updated parameters of the train. The key is FDI. In simulation, this is done following the approach proposed in Section 3.2.2.

In this approach, one employs the algorithm as shown in Figure 3 to detect and identify the fault; this is executed once a second. In the figure, the matrix *Bb* is the coefficient matrix of the brake inputs in the train model, and is equal to $\mathrm{diag}(1/m_i)$ when the braking system is faultless. The variables v_m, v_r are the measured speed and reference speed, respectively. The variable K^f_{brake} is a ten-dimension array used to store the past ten estimated fault signals while N^f_{brake} is a counter number of the continuous violation of fault condition. There are the same possibilities in the FDI of a wagon fault as in the FDI of a sensor fault. Similar to the latter, the FDI of wagon faults is also 'negative feedback' to track the real value of the wagon actuator. The effect of false acceptance on the train performance will not be discussed in a theoretic way, but is discussed with the simulation results. The time delay between the fault occurrence and fault isolation will not be discussed either.

5. Simulation

The simulation setting of the train is the same as in [6] as well as the speed profile and track profile shown in Figure 4. When all sensors and actuators are faultless, the controller is the speed regulator with $K_e = 1, K_f = 1, K_v = 1,$ designed in [6]. The speed regulator is designed in [6] as follows. Step 1: with the reference speed, the optimal equilibrium is calculated with the approach in [34]; Step 2: with the optimal equilibria, the train model is rewritten, and according to this rewritten model, the speed regulator is designed. Here, the reference speed and the coefficients of the sensors and actuators have effects on the equilibria and the rewritten model parameters. Only when the reference speed changes or the fault mode is identified, steps 1 and 2 will be re-processed (redesign the speed regulator).

When a fault occurs, the controller will be redesigned. The controller redesign includes two parts: optimal scheduling and speed regulator.

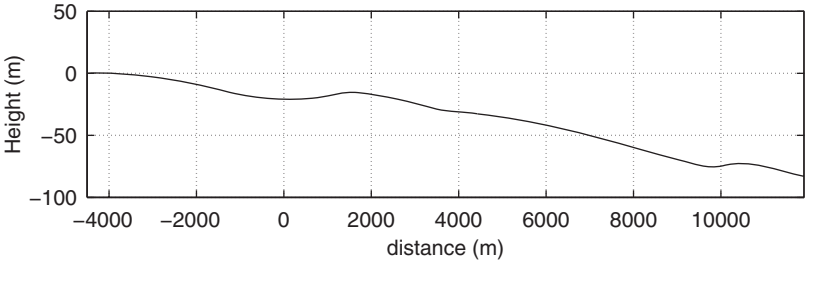

Figure 4. The track profile.

5.1. *Simulation of sensor faults*

In simulation, the sensor FDI program is only working during the cruise phase. The fault diagnosis parameter setting is as in Figure 2.

There are two kinds of errors with the gains of speed sensors. One is a random error, which depends on the accuracy of speed sensor. The other one is a systematic error with gain, which is a real fault and should be corrected. From the simulation, it will be seen that the former has little impact on the performance of controllers, while the latter has much greater impact.

In the following description, the accuracy $1 \pm \alpha\%$ of a speed sensor means the output of the sensor is randomly $1 \pm \alpha\%$ of the measured speed, while the gain fault $\beta\%$ of a sensor means the output of the sensor is $1 + \beta\%$ of the measured speed with the accuracy 1.

The effects of the random errors of the speed sensors on the non-FTC (a controller without fault-tolerant capacity) and the FTC (a controller with fault-tolerant capacity) are discussed firstly. The following three groups of figures are the simulation results with non-FTC of a faultless system, FTC of a faultless system, and FTC of a faulty system, respectively.

Figures 5 and 6 are the simulation results of a faultless system with non-FTC. All sensors in the former case have accuracies of 100%, while those in the latter have accuracies of $1 \pm 5\%$ from the beginning.

Figures 7 and 8 are simulation results of a faultless system with an FTC. All sensors in the former case have accuracies of 100%, while those in the latter have accuracies of $1 \pm 5\%$ from the beginning.

Figures 9 and 10 are the simulation results of a faulty system (the second sensor is faulty with a gain fault $+5\%$). All sensors in the former case have accuracies of 100% while those in the latter have accuracies of $1 \pm 5\%$.

In these figures, the first subplots show the front locomotive group speed, the rear locomotive group speed and the mean speed of all the cars with respect to the distance from the starting point. The second subplots show maximum and minimum in-train forces and the mean value

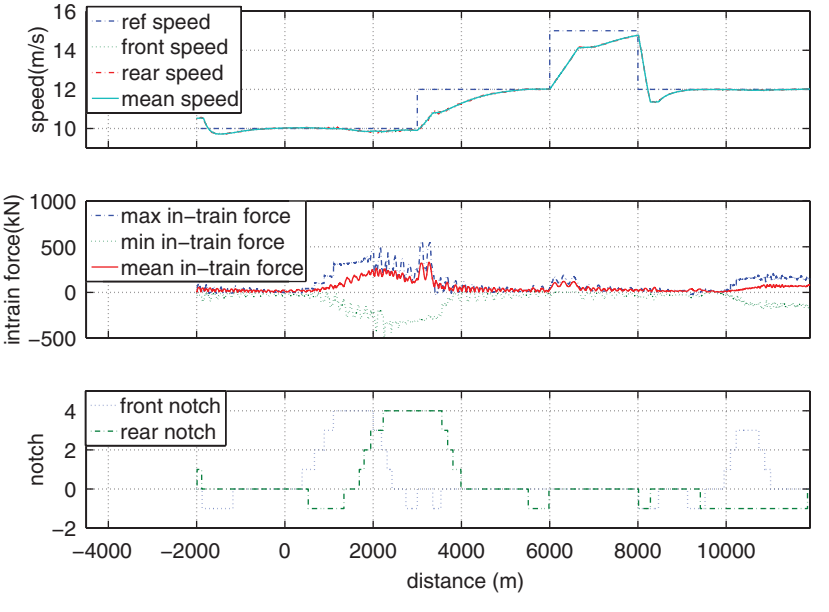

Figure 5. Non-FTC (sensor accuracy of 100%).

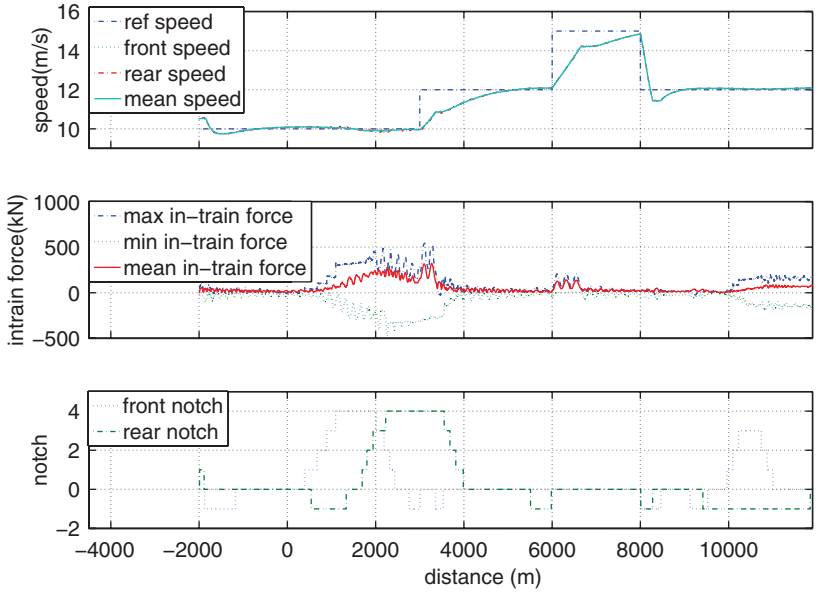

Figure 6. Non-FTC (sensor accuracy of $1 \pm 5\%$).

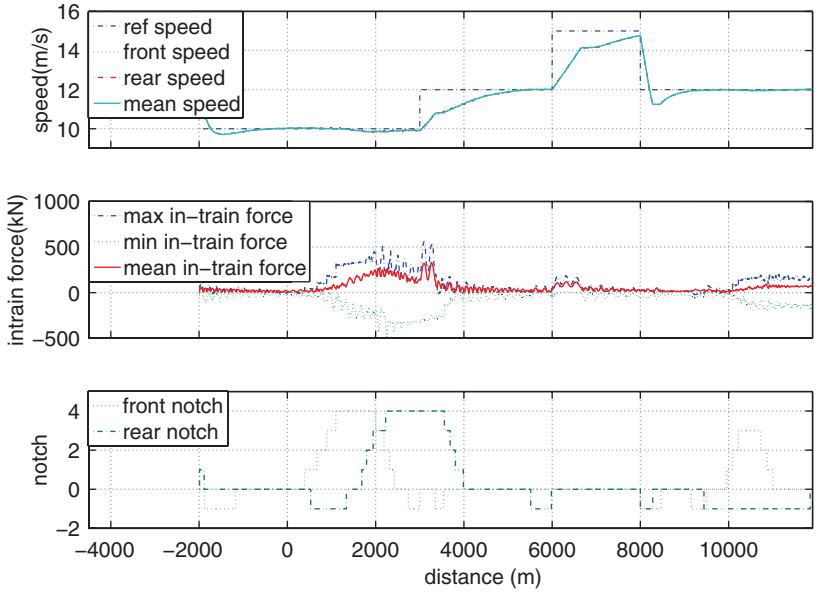

Figure 7. FTC (sensor accuracy of 100%).

of the absolute values of all the in-train forces at a specific time with respect to the distance. The third ones show front and rear locomotive groups' notches along the track.

Comparing Figure 5 with Figure 6, one can see that the random error has very little effect on the speed regulators without fault-tolerant capacity when there is no fault with the sensors. Comparing Figure 7 with Figure 8, it can be seen that the random error makes the performance a little worse with the fault-tolerant controller even though no fault occurs. The effects are,

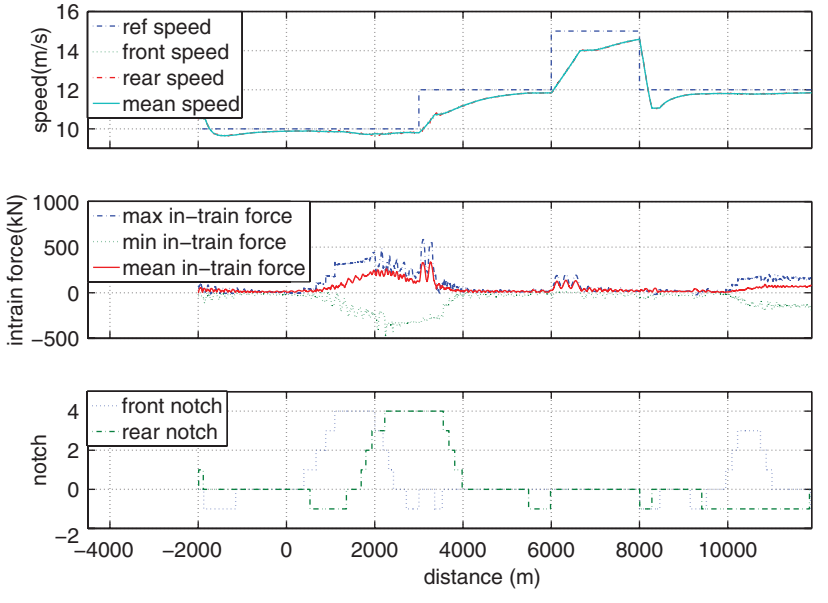

Figure 8. FTC (sensor accuracy of $1 \pm 5\%$).

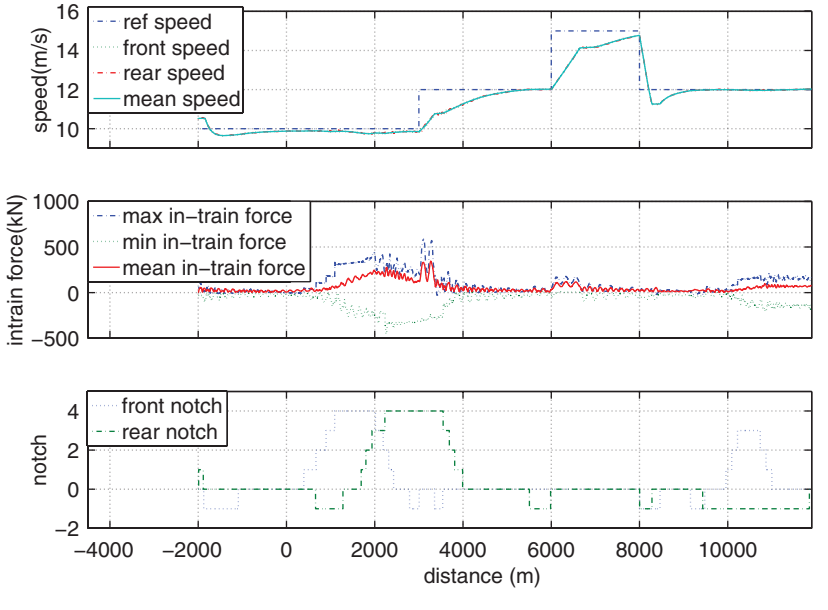

Figure 9. FTC (sensor accuracy of $1 + 0\%$ and second sensor gain fault of $+5\%$).

however, very small. The performance index is referred to in Table 1. From a comparison of Figure 9 with Figure 10, one sees that the random errors of sensors have little impact on the performance of the fault-tolerant controllers when a fault occurs with the second sensor. From a comparison of the last two pairs, it is concluded that random errors have effects on the performance of the fault-tolerant controllers, but the effects are limited. The result is

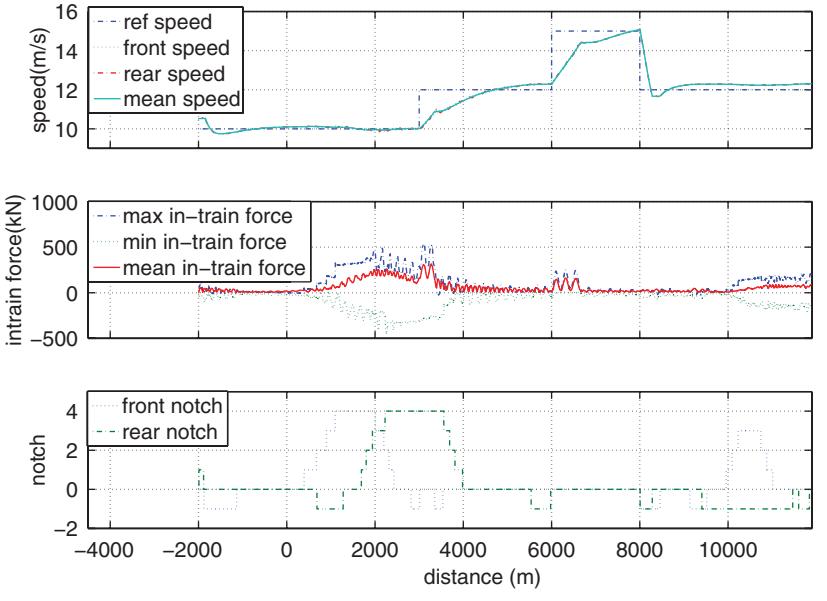

Figure 10. FTC (sensor accuracy of $1 \pm 5\%$ and second sensor gain fault of $+5\%$).

Table 1. Comparison if non-FTC and FTC of sensor faults.

	$\lvert\delta\bar{v}\rvert$(m/s)			$\overline{\lvert f_{\text{in}}\rvert}$(kN)				
	Max	Mean	Std	Max	Mean	Std	E (MJ)	Control type
Figure 5[a]	2.98	0.32	0.53	331.16	58.60	63.05	12,400	non-FTC
Figure 6[b]	2.91	0.32	0.51	323.39	56.46	63.85	12,200	non-FTC
Figure 11[c]	3.53	0.78	0.52	343.89	57.73	63.69	13,100	non-FTC
Figure 10[c]	3.08	0.33	0.47	316.34	59.38	65.03	12,600	FTC
Figure 9[d]	2.98	0.37	0.52	343.37	59.75	63.45	12,900	FTC
Figure 7[a]	2.98	0.33	0.53	331.15	59.51	63.55	12,800	FTC
Figure 8[b]	3.16	0.47	0.52	338.37	55.76	65.51	13,200	FTC
Figure 12[e]	2.98	0.39	0.51	338.72	58.71	64.14	13,000	FTC
Figure 13[f]	2.98	0.51	0.58	328.50	60.50	63.40	12,600	FTC
Figure 14[g]	2.98	0.41	0.51	343.12	58.96	64.13	13,100	FTC
Figure 15[h]	2.98	0.62	0.58	336.38	63.65	62.92	13,400	FTC
Figure 16[h]	3.34	0.60	0.66	345.48	65.65	62.06	13,500	FTC

[a]Faultless, and sensor accuracy 100%.
[b]Faultless, and sensor accuracy $1 \pm 5\%$.
[c]Sensor accuracy $1 \pm 5\%$ and second sensor gain fault $+5\%$.
[d]Sensor accuracy 100% and second sensor gain fault $+5\%$.
[e]Sensor accuracy 100% and third sensor gain fault $+7\%$.
[f]Sensor accuracy 100% and fourth sensor gain fault -20%.
[g]Sensor accuracy 100% and fourth sensor gain fault $+20\%$.
[h]Sensor accuracy 100% and the second sensor gain fault $+30\%$ from the distance of 2000 m and fourth sensor gain fault -30% from the distance of 4000 m.

still acceptable. In the following simulation of this study, one therefore seldom considers the random errors of the sensors. From the above discussion, it is clear the results are not affected.

A discussion of the effects of the FTC on the performance of a speed regulator is as below.

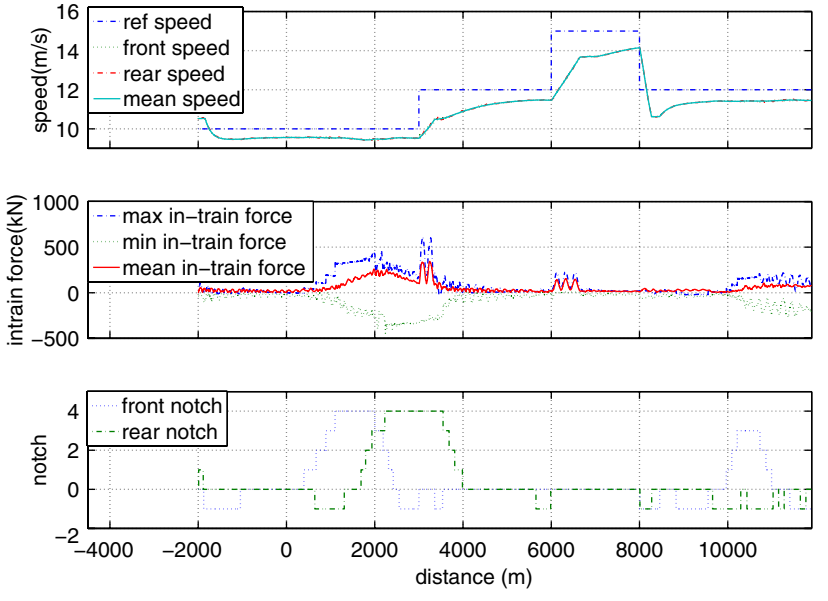

Figure 11. Non-FTC (sensor accuracy of $1 \pm 5\%$ and 2nd sensor gain fault of $+5\%$).

The figures from Figure 5 to Figure 11 are compared. Figure 11 is the simulation result of a faulty system (the second sensor is faulty with a gain fault $+5\%$) with all sensors having accuracies of $1 \pm 5\%$. The controller in this simulation is a non-FTC.

One first compares Figure 5 with Figure 7, in which the sensors have accuracies of 100% and the system is faultless. The former is controlled with a non-FTC while the latter is controlled with an FTC. From these two figures, one can see that the performance is visually very similar although from Table 1 the last one appears to be slightly worse.

Then Figure 6 is compared with Figure 8, in which the sensors have accuracies of $1 \pm 5\%$ and the system is faultless. The former is controlled with a non-FTC while the latter is controlled with an FTC. The speed performance of the latter is a little worse than that of the former, and even the latter has a steady speed error. This is because the random errors of the sensors have an effect on the performance of an FTC. Even so, the FTC does not explicitly worsen the performance of the speed regulator. The result is still acceptable.

The advantage of an FTC can be seen when a fault occurs. Figures 11 and 10 represent simulation of a faulty system (all sensors with accuracies of $1 \pm 5\%$ and the second one has a gain fault of $+5\%$) with a non-FTC and with an FTC, respectively. It is seen that the speed performance of the latter is obviously better than that of the former. That is the contribution of the FTC. From the above comparison, one can conclude that:

(1) When no fault occurs and all sensors have accuracies of 100%, the speed performance of an FTC is very similar to that of a non-FTC.
(2) When no fault occurs and all sensors have accuracies of $1 \pm 5\%$, the speed performance of an FTC is a little worse than that of a non-FTC. However, the result is still thought as a good result.
(3) When a small fault (the second sensor has a gain fault of $+5\%$) occurs and all sensors have accuracies of $1 \pm 5\%$, the speed performance of an FTC is much better than that of a non-FTC.

From the above, it is concluded that the FTC for the sensors' faults is suitable.

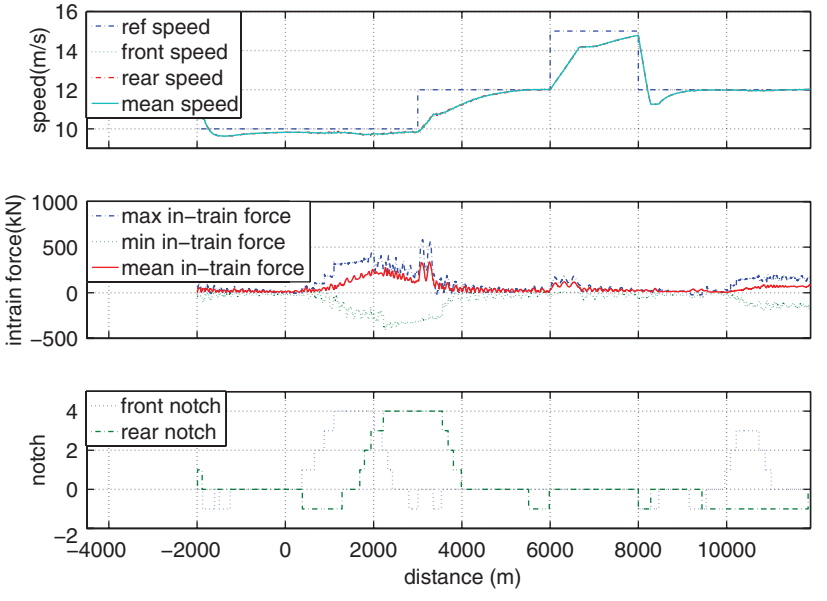

Figure 12. FTC (third sensor with a gain fault of + 7%).

In the above simulations, only the FTC for the second sensor fault is given. In the following, one can see the FTC applied in the faults of the third and fourth sensors, and in the concurrent faults of the second and fourth ones. Since the accuracy of a sensor does not explicitly affect the performance of the controller, without a special description, the sensor accuracy is assumed to be 100% in the rest of this paper.

Figure 12 shows an FTC with the third sensor having a gain fault of + 7% from the beginning. Figure 13 shows an FTC with the fourth sensor having a gain fault of − 20%

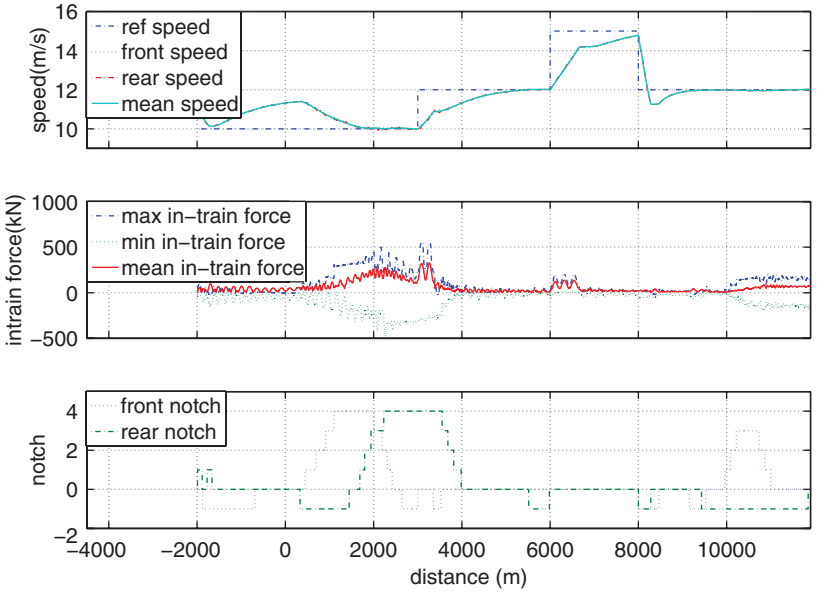

Figure 13. FTC (fourth sensor with a gain fault of − 20%).

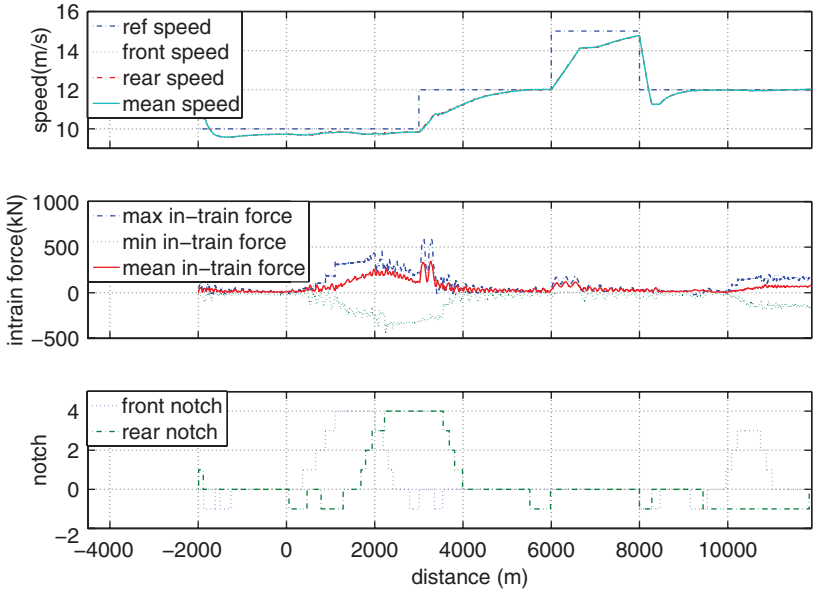

Figure 14. FTC (fourth sensor with a gain fault of + 20%).

from the beginning. Figure 14 shows an FTC with the fourth sensor having a gain fault of + 20% from the beginning.

A kind of concurrent fault (the second sensor has a gain fault of + 43% and the fourth one has a gain fault of + 12% from the beginning) is shown in Figure 15 with an FTC. Another kind of concurrent fault (the second sensor has a gain fault of + 30% from the distance of 2000 m and the fourth one has a gain fault of − 30% from the distance of 4000 m) is shown in Figure 16 with an FTC.

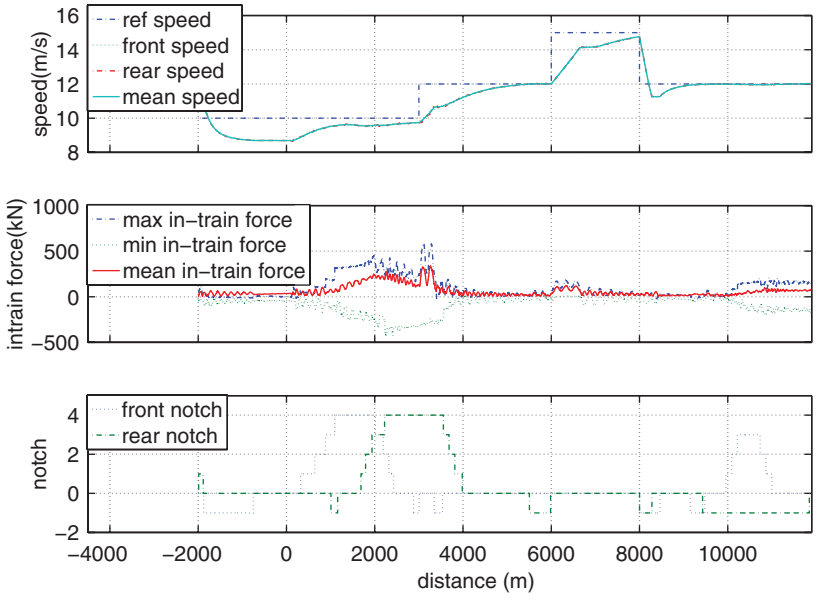

Figure 15. FTC (concurrent faults).

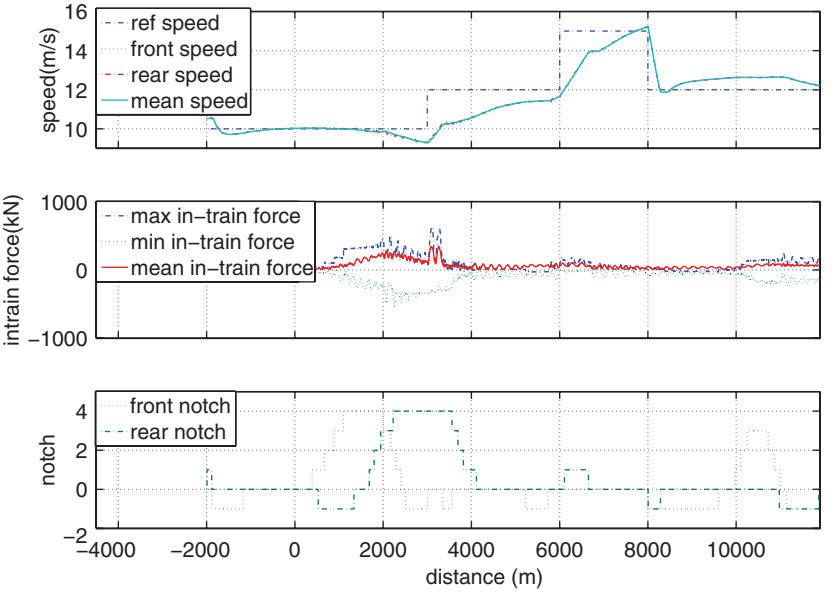

Figure 16. FTC (concurrent faults).

The comparison of these figures in performance is shown in Table 1. $|\delta\bar{v}|$ is the absolute value of the difference between the reference velocity and the mean value of all the cars' velocities at a specific point. $\overline{|f_{\text{in}}|}$ is the mean value of the absolute values of all the couplers' in-train forces at a specific point. The items max, mean, and std are the maximum value, mean value, and standard deviation of the statistical variable. The variable E is the total energy consumption for the track section.

From an analysis of the figures and a comparison with Table 1, one can conclude that the application of FTC of sensor faults in the speed regulation explicitly improves performance in the case of fault occurrence and does not explicitly worsen performance in the case of a faultless train.

5.2. *Simulation of locomotive faults*

In the previous parts, FDI of locomotive faults are assumed to be done by other approaches and only FTC is considered in this paper. The fault signal is assumed to be given when a fault occurs.

In the train setting of simulation, there are two groups of locomotives at the front and at the rear, respectively. Every group is composed of two locomotives. In simulation of an FTC, one assumes that the fault is one locomotive in a locomotive group that does not work. When the two locomotives in a group do not work, distributed power control cannot apply, which is not discussed in this study. So, in the simulation, it is assumed that the fault is detected 60 s after it happens and the controller is then redesigned. There are three types of faults:

(1) Front-loco-fault: one locomotive of the front locomotive group does not work.
(2) Rear-loco-fault: one locomotive of the rear locomotive group does not work.
(3) Both-loco-fault: one locomotive of the front locomotive group and one of the rear group do not work.

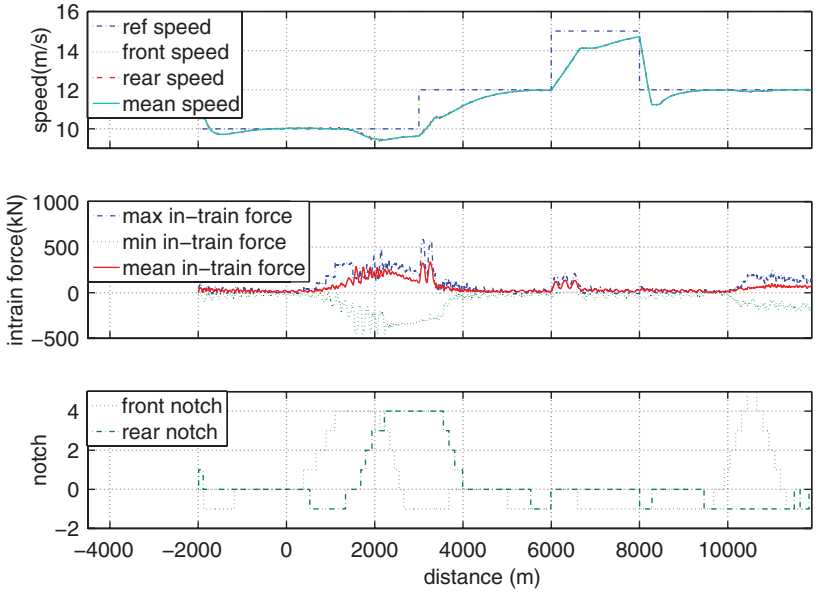

Figure 17. Front-loco-fault with an FTC.

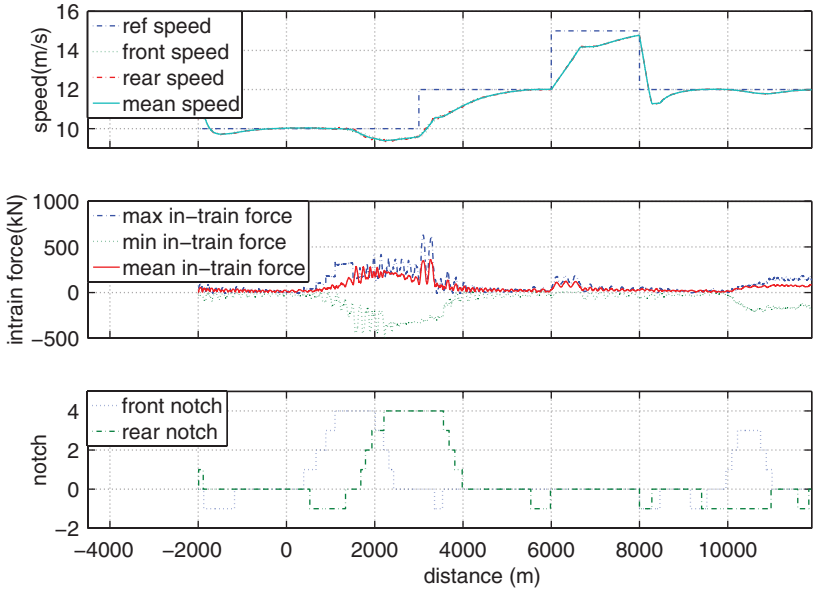

Figure 18. Front-loco-fault with a non-FTC.

Figures 17 and 18 are simulation results of Front-loco-fault with an FTC and a non-FTC, respectively. One of the locomotives at the front does not work from the distance 1500 m.

Figures 19 and 20 are simulation results of rear-loco-fault with an FTC and a non-FTC, respectively. One of the locomotives at the rear does not work from the distance 1500 m.

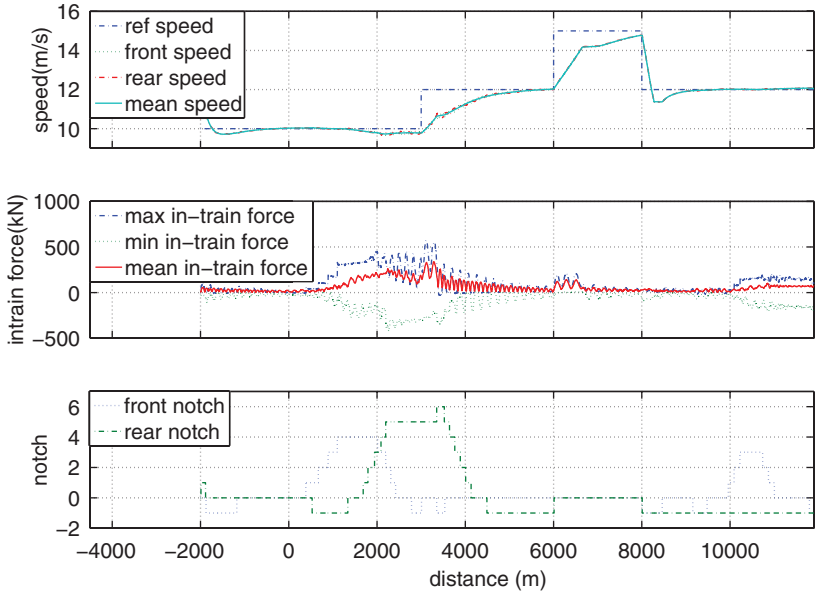

Figure 19. Rear-loco-fault with an FTC.

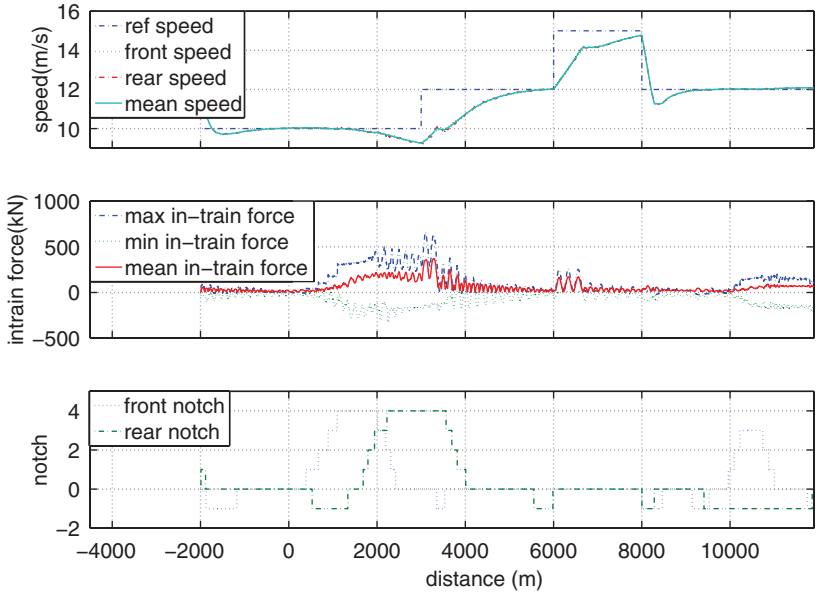

Figure 20. Rear-loco-fault with a non-FTC.

Figures 21 and 22 are simulation results of Both-loco-fault with an FTC and a non-FTC, respectively. One locomotive at the front and one at the rear do not work from the distance 1500 m.

From comparing Figures 17 and 18, it can be seen that the performance of an FTC is better than that of a non-FTC during the period when the train is passing over a hill. (In these figures, the track profile is the same as that of previous simulation and is not shown.) That can also be

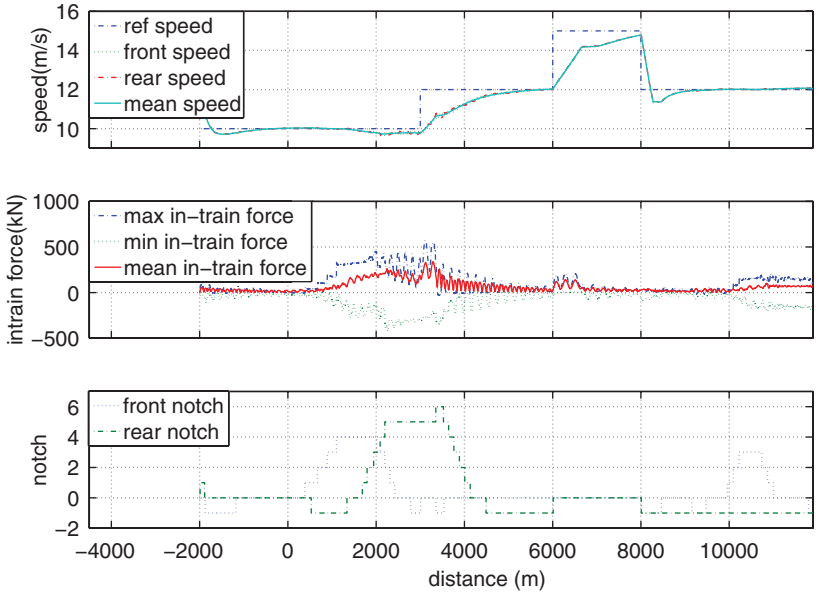

Figure 21. Both-loco-fault with an FTC.

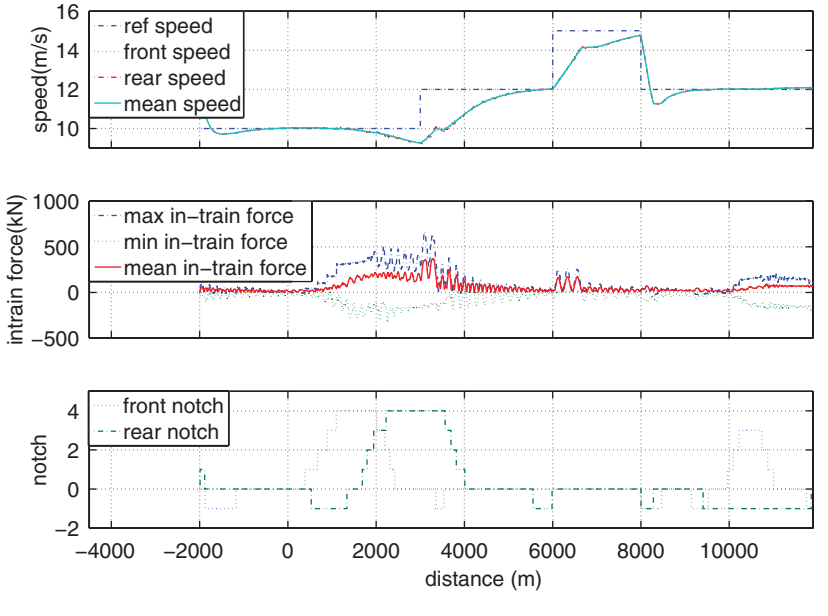

Figure 22. Both-loco-fault with a non-FTC.

seen from the front locomotive effort. When the effort of the front locomotive group is zero, then there is no difference between the FTC and non-FTC. When the front locomotive group uses traction power, the speed performance of the FTC is better.

The above conclusion is also clear from a comparison of Figure 19 with Figure 20, and Figure 21 with Figure 22. The performance comparison of these figures is shown in Table 2.

Table 2. Comparison of non-FTC and FTC of locomotive faults.

	$\lvert\delta\bar{v}\rvert$(m/s)			$\overline{\lvert f_{\text{in}}\rvert}$(kN)				
	Max	Mean	Std	Max	Mean	Std	E (MJ)	Control types
Figure 17[a]	3.03	0.41	0.56	338.40	56.57	65.32	11,600	FTC
Figure 18[a]	2.99	0.41	0.55	361.80	60.19	65.19	10,800	non-FTC
Figure 19[b]	2.98	0.35	0.54	339.61	64.53	63.98	12,200	FTC
Figure 20[b]	2.98	0.45	0.65	372.29	64.31	65.98	9,680	non-FTC
Figure 21[c]	3.02	0.42	0.57	370.39	60.00	64.87	11,400	FTC
Figure 22[c]	3.17	0.54	0.73	355.97	58.80	66.31	7,800	non-FTC

[a]One of the two locomotives at the front does not work from the distance of 1500 m.
[b]One of the two locomotives at the rear does not work from the distance of 1500 m.
[c]One locomotive at the front and one at the rear do not work from the distance of 1500 m.

The advantage of an FTC in the locomotive fault does not seem obvious during most of the simulation period. This is because the locomotive groups make no effort (not powered) during most of the travel period. When the locomotive groups make efforts, the advantage is obvious.

5.3. *Simulation of wagon faults*

In previous sections, an approach to calculate the steady-state speed difference as an FDI of the wagons' brake fault was proposed. In simulation, all faults occur from the distance 1500 m. The simulation results are shown below.

Figure 23 depicts the simulation of an FTC of the wagon braking system with a faultless system. The corresponding simulation of a non-FTC is shown in Figure 24. In comparing these two figures, one can see that the FTC does not explicitly worsen the performance of the speed regulator.

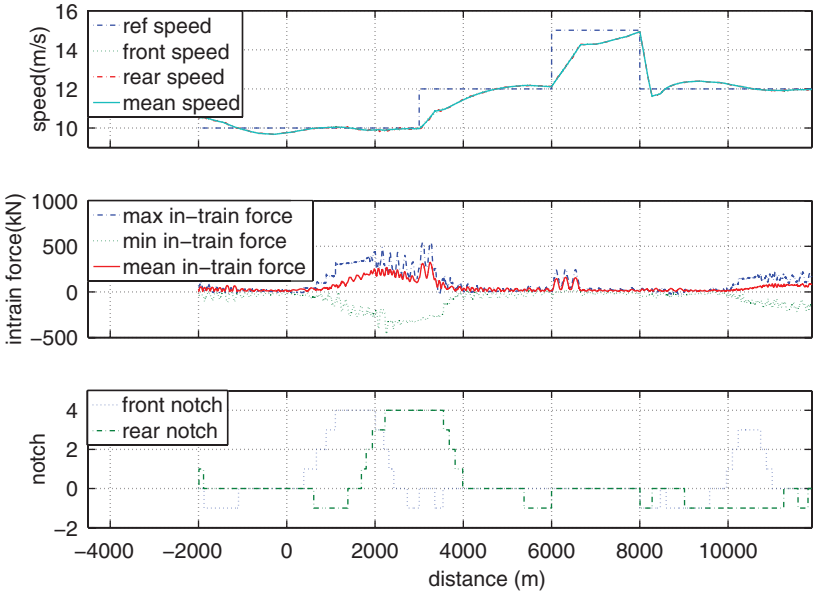

Figure 23. Faultless train with an FTC of braking system.

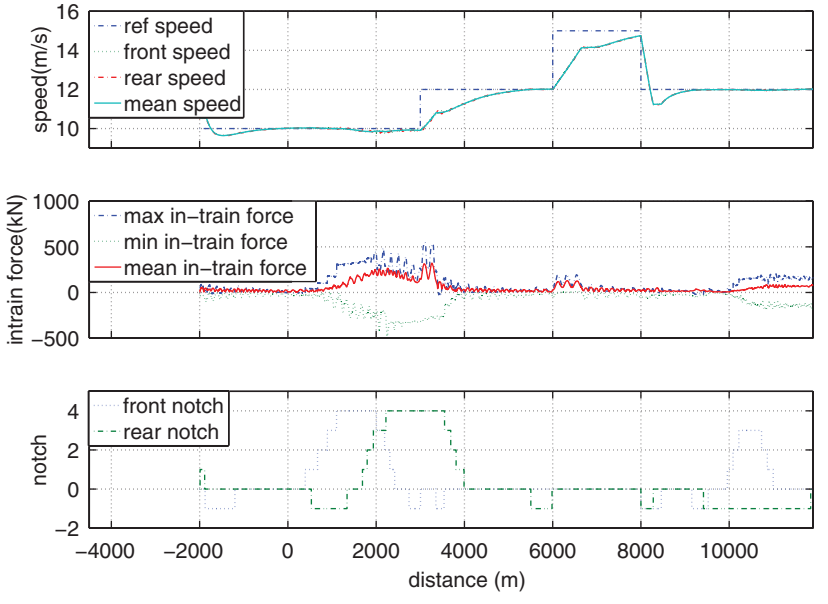

Figure 24. Faultless train with a non-FTC of braking system.

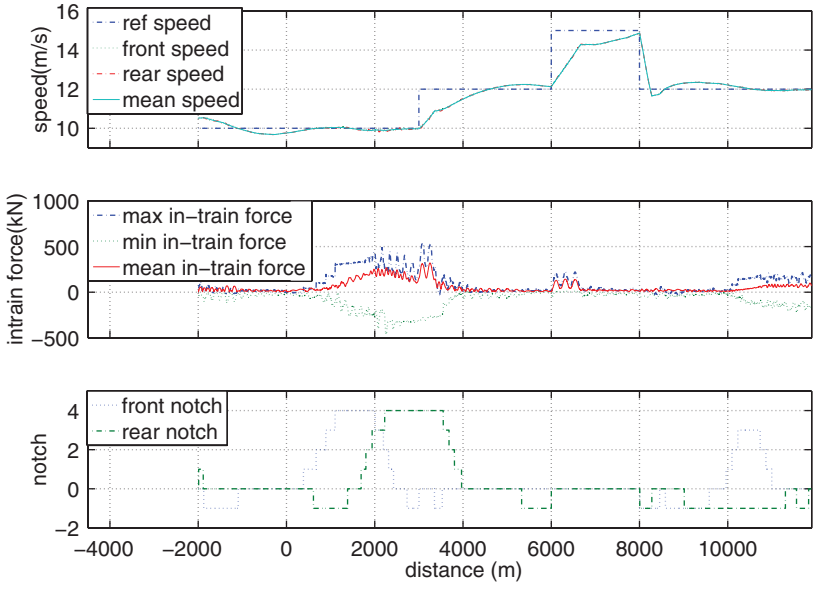

Figure 25. Small fault in an FTC of braking system.

Figures 25 and 26 represent the simulation results of an FTC and a non-FTC when the braking system makes only 97% of the expected braking efforts. This fault is very small. From a comparison of the FTC and the non-FTC, the difference between them is very small. Also from comparing Figure 25 with Figure 23, one knows such a small fault does not affect the performance of the speed regulator.

When a more serious fault occurs (the braking system makes 70% of the expected braking efforts), the difference between the FTC and the non-FTC is obvious, which can be seen from

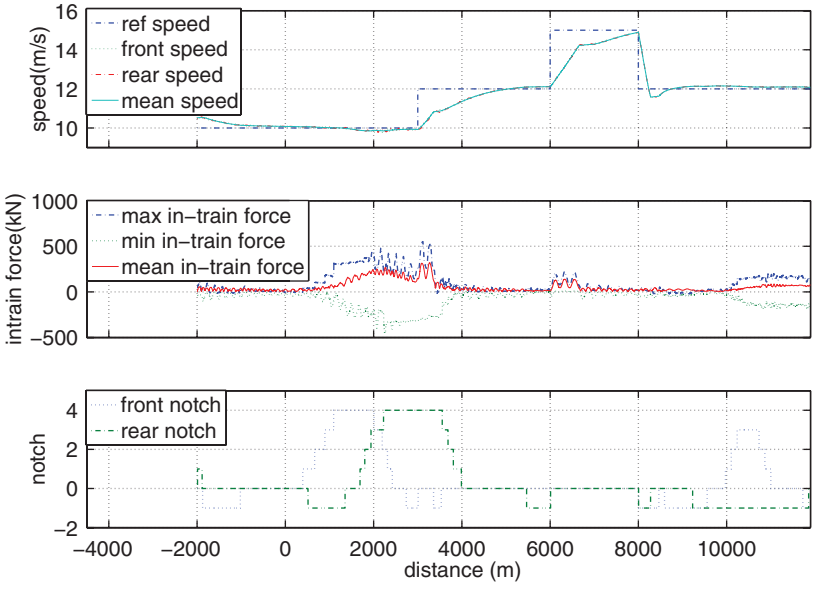

Figure 26. Small fault in a non-FTC.

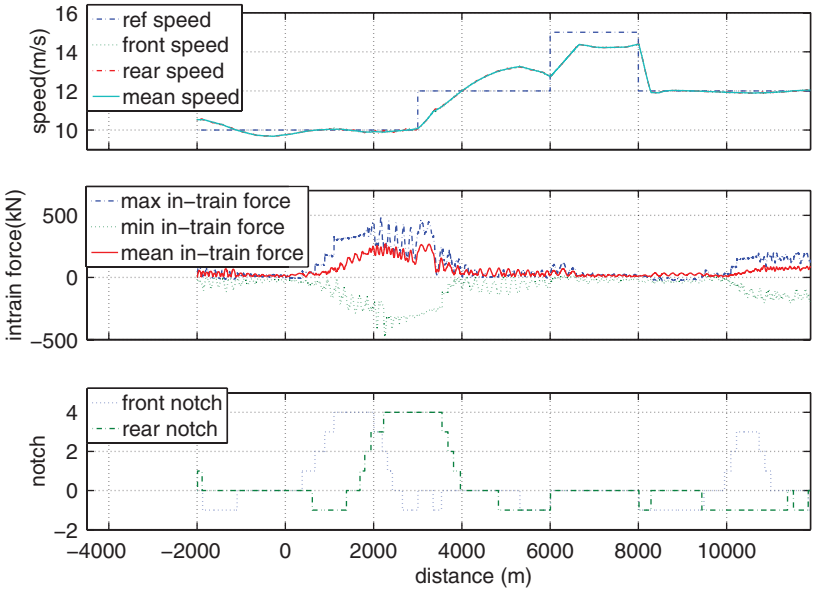

Figure 27. Big fault in an FTC of braking system.

a comparison of Figure 27 with Figure 28. The former is with an FTC and the latter with a non-FTC.

When only part of the braking efforts are faulty (the braking efforts of 2nd to 31st wagon groups are 70% of the expected from the distance 1500 m) the performance of an FTC is also better than that of a non-FTC, although the FTC is designed for the whole braking system, which can be seen from a comparison of Figure 29 with Figure 30. The performance comparison is shown in Table 3.

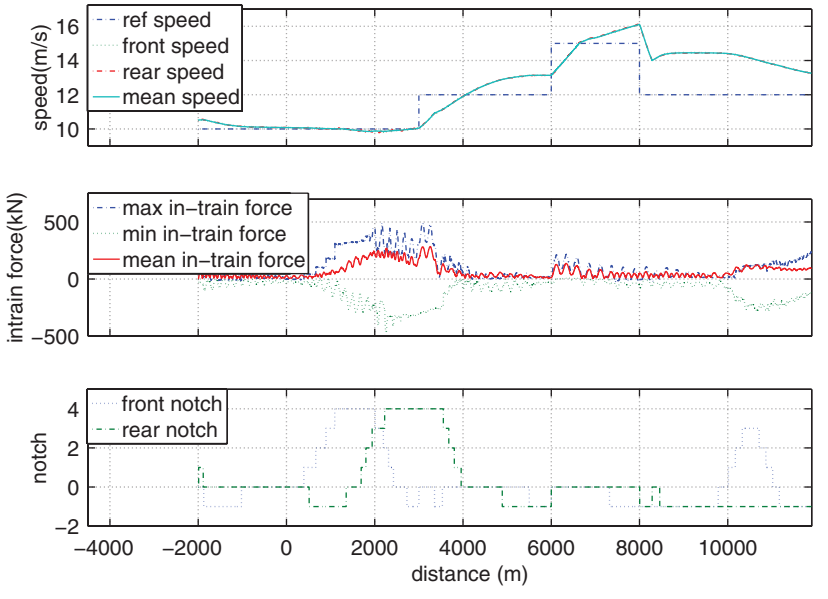

Figure 28. Big fault in a non-FTC.

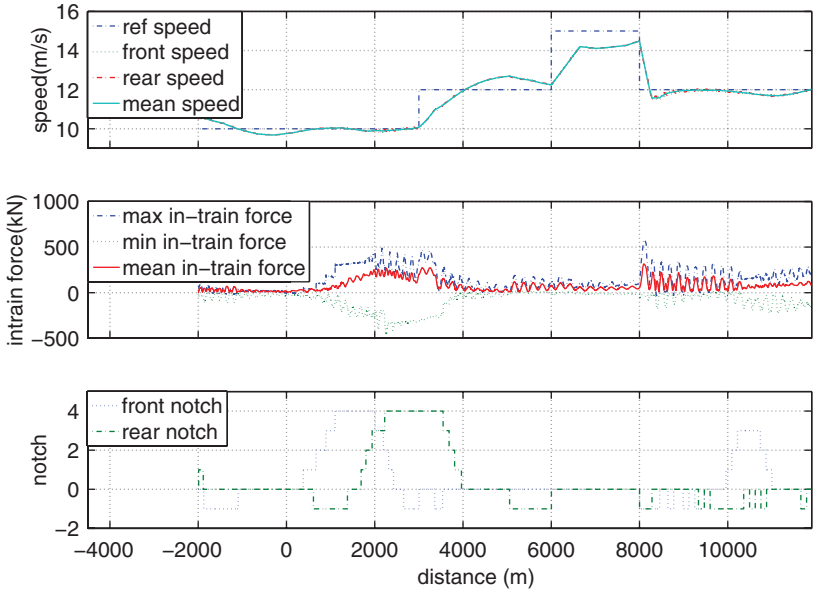

Figure 29. Partial fault in an FTC of braking system.

From the above comparison, one can draw the following conclusions:

(1) A small fault in the braking system has very little effect on the performance of the speed regulator.
(2) The application of an FTC together with a speed regulator does not explicitly worsen the performance of the speed regulator when the system is faultless.

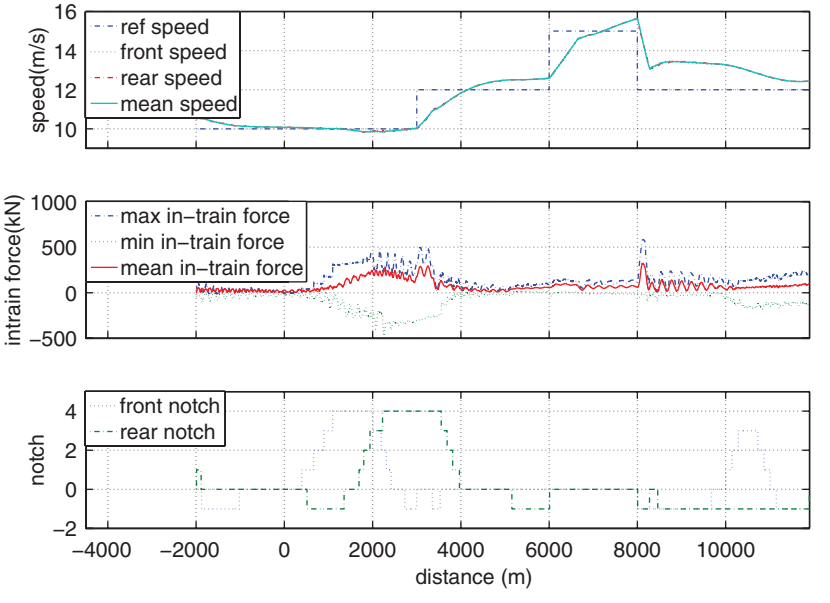

Figure 30. Partial fault in a non-FTC.

Table 3. Comparison of non-FTC and FTC of wagon faults.

	$\lvert\delta\bar{v}\rvert$(m/s)			$\overline{\lvert f_{\text{in}}\rvert}$(kN)				
	Max	Mean	Std	Max	Mean	Std	E (MJ)	Control type
Figure 23[a]	2.92	0.35	0.49	323.89	56.64	63.99	12,300	FTC
Figure 24[a]	2.99	0.41	0.55	361.80	60.19	65.19	10,800	Non-FTC
Figure 25[b]	2.87	0.35	0.48	321.31	55.86	63.70	12,300	FTC
Figure 26[b]	2.89	0.33	0.50	321.64	56.79	63.51	12,299	Non-FTC
Figure 29[c]	2.76	0.37	0.47	315.71	78.30	66.15	12,256	FTC
Figure 30[c]	3.64	0.53	0.56	322.02	75.93	63.79	11,957	Non-FTC

[a]Faultless.
[b]The braking effort is 97% of the expected.
[c]The braking efforts of 2nd to 31st wagon group are 70% of the expected from the distance of 1500 m.

(3) When a small fault occurs, there is little difference between the application of an FTC and a non-FTC.
(4) The application of an FTC can improve the performance when a big fault of the braking system occurs.
(5) Even if a fault occurs in part of the braking system, which is different from the assumed fault mode as in Equation (7) (fault with the whole braking system), the application of an FTC can improve the performance of the speed regulator.

6. Conclusion

In this paper, the FTC of heavy-haul trains is discussed. The discussion is based on the redesign of the speed regulator with measurement feedback proposed in [6].

The FDIs for the gain faults of the sensors and the braking system are respectively studied, while the FDI of the locomotive fault is not studied, but the latter can be done following some other approaches, such as one proposed in [27]. The FDI of sensor faults is based on a geometric approach proposed in [21]. The FDI of a braking system is based on the observation of the steady-state speed. From the difference of the steady speeds between the fault system and the faultless system, one can get the fault information.

These two kinds of FDIs are studied separately, and need to be studied further together. In the opinion of the authors, it is possible to apply them together, because the FDI of a sensor fault is based on the difference between the measured speed of a sensor and the estimated speed of the observer, while the FDI of a braking fault is based on the difference between the measured speeds (steady-state speeds) and the reference speed. In the former, a necessary condition for the diagnosis of a fault is that there are differences among the measured speeds while in the latter, a necessary condition for a diagnosis of a fault is that there are nearly no differences among the measured speeds (because a steady state is assumed). This is, however, just a theoretical discussion. In fact, because of the accuracy of the sensor and the ideal assumption of a steady state, the visibility of the difference of the measured speeds depends on a threshold. The choice of the threshold affects the performance of the two FDIs, which is not discussed in this paper.

Simulation tests were conducted on the suitability of the two FDIs and the redesign of speed regulators according to the fault signals from the FDIs of sensor faults and braking system faults, and the FDI (not included in this study) of locomotive faults.

Simulation shows that the random errors of the speed sensors have very little impact on the train's performance. It is also shown that the proposed FTC does not explicitly worsen the performance of the speed regulator in the case of a faultless system, while it obviously improves the performance of the speed regulator in the case of a faulty system.

Notation

m	mass of a car, which may be a wagon or a locomotive
v_i	the ith car's speed
x_i	the relative distance of the neighbouring cars
f_{a_i}	the force undertaken by the ith car from the environment
f_{aero_i}	the ith car's aerodynamic force
f_{p_i}	the force undertaken by the ith car due to the car's position
f_{in_i}	the in-train force between the ith and $(i+1)$th cars
c_{0i}, c_{1i}, c_{2i}	the aero-dynamical coefficients
v_r	the reference speed, i.e., speed tracking command
δx	the difference of the variable x from the equilibria x_0
$\dot{x}$	the differential of x with respect to t
v_i	the sensor output for the ith car's speed
v_i^o	the real speed of the ith car
ls_i	the number of the car which is equipped with the speed sensor numbered as i
$m_{v_i}^f$	the constant gain fault of the sensor for ith car
v_{ls_i}	the output of the ith speed sensor
$m_{v_{ls_i}}^f$	the constant gain fault of the ith speed sensor
u_i	is the expected output of ith actuator
u_i^f	is the real output of the ith actuator
$m_f^{l_i}$	the fault coefficient for the ith locomotive effort
m_f^w	the fault coefficient for the ith wagon braking effort

References

[1] J. Cheng and P. Howlett, *Application of critical velocities to minimization of fuel consumption in the control of trains*, Automatica 28(11) (1992), pp. 165–169.
[2] J. Cheng and P. Howlett, *A note on the calculation of optimal strategies for the minimization of fuel consumption in the control of trains*, IEEE Trans. Automat. Control 38(11) (1993), pp. 1730–1734.
[3] A. Astolfi and L. Menini, *Input/output decoupling problem for high speed trains*, Proc. Amer. Control Conf. 1 (2002), pp. 549–554.
[4] C. Yang and Y. Sun, *Robust cruise control of high speed train with hardening/softening nonlinear coupler*, Proc. Amer. Control Conf. 3 (1999), pp. 2200–2204.
[5] C. Yang and Y. Sun, *Mixed H_2/H_∞ cruise controller design for high speed train*, Int. J. Control 74(9) (2001), pp. 905–920.
[6] X. Zhuan and X. Xia, *Speed regulation with measured output feedback in the control of heavy haul trains*, Automatica 44(1) (2008), pp. 242–247.
[7] M. Chou, X. Xia, and C. Kayser, *Modelling and model validation of heavy-haul trains equipped with electronic controlled pneumatic brake systems*, Control Eng. Practice 15(4) (2007), pp. 501–509.
[8] P.M. Frank, *Fault diagnosis in dynamic systems using analytical and knowledge-based redundancy – a survey and some new results*, Automatica 26(3) (1990), pp. 459–474.
[9] P.M. Frank, *On-line fault detection in uncertain nonlinear systems using diagnostic observers: a survey*, Int. J. Systems Sci. 25(12) (1994), pp. 2129–2154.
[10] R.J. Patton, *The 1997 situation (survey)*, Proceedings of the IFAC Symposium SAFE PROCESS'97, Vol. 2, The University of Hull, August 26–28, 1997, pp. 1033–1055.
[11] R. Isermann, *Fault diagnosis of machines via parameter estimation and knowledge processing – tutorial paper*, Automatica 29(4) (1993), pp. 815–835.
[12] E.A. García and P.M. Frank, *Deterministic nonlinear observer-based approaches to fault diagnosis: a survey*, Control Eng. Practice 5(5) (1997), pp. 663–670.
[13] M. Blanke, R. Izadi-Zamanabadi, S.A. Bϕgh, and C.P. Lunau, *Fault-tolerant control systems – a holistic view*, Control Eng. Practice 5(5) (1997), pp. 693–702.
[14] R. Isermann, *Supervision, fault-detection and fault-diagnosis methods an introduction*, Control Eng. Practice 5(5) (1997), pp. 639–652.
[15] R. Isermann, *Model-based fault-detection and diagnosis – status and applications*, Annu. Rev. Control 29(1) (2005), pp. 71–85.
[16] M.A. Massoumnia, G.C. Verghese, and A.S. Willsky, *Failure detection and identification*, IEEE Trans. Automat. Control 34(3) (2005), pp. 316–321.
[17] M. Basseville, *Information criteria for residual generation and fault detection and isolation*, Automatica 33(5) (1997), pp. 783–803.
[18] H. Hammourie, P. Kabore, and M. Kinnaert, *A geometric approach to fault detection and isolation for bilinear systems*, IEEE Trans. Automat. Control 46(9) (2001), pp. 1451–1455.
[19] Q. Zhang, M. Basseville, and A. Benveniste, *Fault detection and isolation in nonlinear dynamic systems: a combined input-output and local approach*, Automatica 34(11) (2001), pp. 1359–1373.
[20] H. Hammouri, M. Kinnaert, and E.H.E. Yaagoubi, *Observer-based approach to fault detection and isolation for nonlinear systems*, IEEE Trans. Automat. Control 44(10) (1999), pp. 1879–1884.
[21] C. De Persis and A. Isidori, *A geometric approach to nonlinear fault detection and isolation*, IEEE Trans. Automat. Control 46(6) (2001), pp. 853–865.
[22] C.De Persis and A. Isidori, *On the observability codistributions of a nonlinear system*, Systems Control Lett. 40(5) (2000), pp. 297–304.
[23] Z. Qu, C.M. Ihlefeld, Y. Jin, and A. Saengdeejing, *Robust fault-tolerant self-recovering control of nonlinear uncertain systems*, Automatica 39(10) (2003), pp. 1763–1771.
[24] X. Zhang, T. Parisini, and M.M. Polycarpou, *Adaptive fault-tolerant control of nonlinear uncertain systems – an information-based diagnostic approach*, IEEE Trans. Automat. Control 49(8) (2004), pp. 1259–1274.
[25] A. Xu and Q. Zhang, *Nonlinear system fault diagnosis based on adaptive estimation*, Automatica 40(7) (2004), pp. 1181–1193.
[26] R. Mattone and A.D. Luca, *Relaxed fault detection and isolation: an application to a nonlinear case study*, Automatica 42(1) (2006), pp. 109–116.
[27] S. Daley, D.A. Newton, S.M. Bennett, and R.J. Patton, *Methods for fault diagnosis in rail vehicle traction and braking systems*, IEE Colloquium on Qualitative and Quantitative Modelling Methods for Fault Diagnosis, London, UK. April 24, 1995, pp. 5/1–5/13.
[28] S.M. Bennett, R.J. Patton, and S. Daley, *Sensor fault-tolerant control of a rail traction drive*, Control Eng. Practice 7(2) (1999), pp. 217–225.
[29] A. Schwarte, F. Kimmich, and R. Isermann, *Model-based fault detection and diagnosis for diesel engines*, MTZ Worldwide 63 (2002), pp. 612–620.
[30] F. Kimmich, A. Schwarte, and R. Isermann, *Fault detection for modern diesel engines using signal- and process model-based methods*, Control Eng. Practice 13(2) (2005), pp. 189–203.
[31] C. Bonivento, A. Isidori, L. Marconi, and A. Paoli, *Implicit fault-tolerant control: application to induction motors*, Automatica 40(3) (2004), pp. 355–371.

[32] X. Zhuan, *Fault-tolerant control of heavy haul trains*, Proceedings of the 7th IFAC Symposium on Nonlinear Control Systems, Pretoria, South Africa, August 22–24, 2007.
[33] X. Zhuan and X. Xia, *Cruise control scheduling of heavy haul trains*, IEEE Trans. Control System Technol. 14(4) (2006), pp. 757–766.
[34] X. Zhuan and X. Xia, *Optimal scheduling and control of heavy haul trains equipped with electronically controlled pneumatic braking systems*, IEEE Trans. Control System Technol. 15(16) (2007), pp. 1159–1166.